Hindawi Advances in Meteorology Volume 2020, Article ID 4230627, 14 pages https://doi.org/10.1155/2020/4230627



Research Article

Meteorological Analysis of Floods in Ghana

S. O. Ansah , M. A. Ahiataku, C. K. Yorke, F. Otu-Larbi, Bashiru Yahaya, P. N. L. Lamptey, and M. Tanu

¹Ghana Meteorological Agency, Accra, Ghana

Correspondence should be addressed to S. O. Ansah; ansahsamuelowusu2014@gmail.com

Received 12 September 2019; Revised 5 January 2020; Accepted 30 January 2020; Published 24 March 2020

Academic Editor: Eduardo García-Ortega

Copyright © 2020 S. O. Ansah et al. This is an open access article distributed under the Creative Commons Attribution License, which permits unrestricted use, distribution, and reproduction in any medium, provided the original work is properly cited.

The first episodes of floods caused by heavy rainfall during the major rainy season in 2018 occurred in Accra (5.6°N and 0.17°W), a coastal town, and Kumasi (6.72°N and 1.6°W) in the forest region on the 18th and 28th of June, respectively. We applied the Weather Research and Forecasting (WRF) model to investigate and examine the meteorological dynamics, which resulted in the extreme rainfall and floods that caused 14 deaths, 34076 people being displaced with damaged properties, and economic loss estimated at \$168,289 for the two cities according to the National Disaster Management Organization (NADMO). The slow-moving thunderstorms lasted for about 8 hours due to the weak African Easterly Wave (AEW) and Tropical Easterly Jet (TEJ). Results from the analysis showed that surface pressures were low with significant amount of moisture influx aiding the thunderstorms intensification, which produced 90.1 mm and 114.6 mm of rainfall over Accra and Kumasi, respectively. We compared the rainfall amount from this event to the historical rainfall data to investigate possible changes in rainfall intensities over time. A time series of annual daily maximum rainfall (ADMR) showed an increasing trend with a slope of 0.45 over Accra and a decreasing trend and a slope of -0.07 over Kumasi. The 95th percentile frequencies of extreme rainfall with thresholds of 45.10 mm and 42.16 mm were analyzed for Accra and Kumasi, respectively, based on the normal distribution of rainfall. Accra showed fewer days with more heavy rainfall, while Kumasi showed more days with less heavy rainfalls.

1. Introduction

Floodis a major hazard and source of human vulnerability which can lead to high mortality rate. Other impacts include outbreak of diseases, disruption of energy supply, communication, and transport infrastructure, and interference in public service delivery. The African continent is the second hardest hit by floods in terms of number of events, area affected, and number of people killed after Asia [1, 2]. Flash floods are frequent across the continent resulting from intense localized thunderstorm activity, slow-moving thunderstorms, or squall lines mostly accompanied by lightning [3]. Various countries in Africa have experienced flood-related disasters in the recent past. In February and March 2000, Mozambique experienced heavy rains and cyclones that caused the worst flooding in 50 years, which led to widespread devastation in some cities [4]. Over 500 lives were also lost and several thousands were forced to

migrate to other communities after a 2007 flood event that affected Uganda, Ethiopia, Sudan, Togo, Mali, Niger, and Burkina Faso, which displaced millions of people [5].

Floods in West Africa in 2009 after torrential rains affected 600,000 people in sixteen West African countries [6]. The most affected countries were Burkina Faso, Senegal, Niger, and Ghana. In 2012, Nigeria experienced one of the most devastating flooding events ever recorded [7]. This flooding incident led to the deaths and displacement of 363 and 2.3 million people, respectively, and the destruction of 59,000 houses and also affected large tracts of farmland and livestock.

Urban flooding has been a frequent occurrence in Ghana since 1930 [8]. At least 18 out of the last 50 years have recorded significant flooding incidences in which lives and properties have been lost [8–11]. Since 1995, the frequency of flooding has increased in the coastal areas of Ghana [4]. The same study found that the ability of people

²Ghana Space Science and Technology Institute, Ghana Atomic Energy Commission, Kwabenya, Ghana

to prepare for possible floods had become more difficult due to increasing variability in rainfall patterns. Flooding in Ghana often occurs in the aftermath of intense and/or continuous rainfall, which results in high run-offs. Possible reasons given for occasional flooding in Ghana include climate variability and change [10, 12] and poor physical planning and flaws in the drainage network [8]. Flooding is ranked the second highest natural disaster after epidemics in Ghana according to [13]. Between the years 1900 and 2014, the economic loss as a result of flooding was approximately US\$ 780,500,000 [14].

2

The most devastating flooding event in Ghanaian history occurred on the 3rd of June 2015, when most parts of southern Ghana experienced heavy thunderstorms and rain. The active spot of the storm was centered over Accra, where 212.8 mm of rainfall was recorded leading to flooding over many areas in the city. This flooding incident and an explosion of a fuel filling station at Kwame Nkrumah Circle, a suburb of Accra, claimed over 150 lives and destroyed lots of properties while displacing hundreds of people.

Various studies have looked at different aspects of rainfall over the West African region in general and Ghana in particular. These include studies focusing on dynamics of the West African Monsoon [15] and onset, cessation, and length of rainfall season [16–18]. The potential impact of climate change on precipitation and weather patterns over West Africa has also been extensively studied (e.g., see [19–23]). These studies have identified and explained the roles of key drivers of variability in West African rainfall such as the Madden Julian Oscillation [24], the movement of the intertropical convergence zone [25, 26], the African Easterly Jet and African Easterly Wave [27, 28], and El Niño-Southern Oscillation [29, 30].

On the contrary, there are very few case studies focusing on the meteorological dynamics of heavy precipitation events within the rainfall season, although there are studies on the impacts such weather events have on livelihoods and society (e.g., see [8, 14]). One of the reasons for the limited research on extreme rainfall in West Africa is the difficulty in accessing data [31]. However, a case study by [32] identified La Nina event in the tropical Pacific, anomalous heating in the tropical Atlantic, and enhanced activity of African easterly waves as possible causes of anomalous heavy precipitation and flooding over sub-Saharan Africa in 2007.

In addition to the factors identified by Paeth et al. [32], the occurrence of heavy rainfall also depends on mesoscale and localized convective processes. These convective processes are influenced by the topography, vegetation cover, and water bodies as well as land surface energy fluxes. Understanding the dynamics of meteorological conditions and features that influence heavy rainfall will greatly improve extreme weather forecasts and help to mitigate their effect. Early identification of meteorological features that could lead to extreme weather event such as torrential rain can help inform early warning systems, which will reduce fatalities and the economic losses.

On the 18th and 28th of June 2018, heavy rains and thunderstorms caused flooding in the two biggest cities in

Ghana, resulting in the deaths of 14 people, displacement of 34,076 others, and damaged properties estimated at \$168,289 according to the National Disaster Management Organization (NADMO). The heavy rainfall events afford us the opportunity to conduct a unique case study focusing on the meteorological explanation of the causes of the event. The aim of this paper is to document the meteorological conditions that led to the initiation and propagation of the weather systems that caused the heavy precipitation events in Accra and Kumasi by analyzing the synoptic and mesoscale weather charts. The study area and data are described in Section 2. Section 3 provides meteorological analysis and discussion. The key conclusions from the results and analysis are presented in Section 4.

2. Materials and Methods

2.1. Study Area. Ghana is a tropical West African country located between latitudes 4°N to 12°N and longitudes 1.5°E to 3.5°W. Its climate is dominated by the wet and the dry seasons. These seasons are modulated by the intertropical boundary (ITB) and the two main high-pressure systems, namely, St. Helena high-pressure system located in the Southern hemisphere and the Azores high-pressure system located over the Atlantic Ocean. Mechanisms of how the ITB and high pressure systems affect rainfall patterns over West Africa are explained in various literatures [16, 33-36]. The wet season is characterized by the intensification of the St. Helena high-pressure system, which induces moisture influx into the country through the south westerly (SW) winds (maritime air mass) which is the major wind that prevails during this season. The intensification of the Azores highpressure system with the north easterly (NE) winds (continental air mass) dominating induces dryness and dust particles over the country during the dry season. The northward and the southward oscillation of the ITB control the rainfall pattern in Ghana where the southern half (below 9°N) of the country experiences bimodal rainfall pattern. April to July is classified as the major rainy season and September to November is the minor rainy season. In this study, two flood cases that occurred on the 18th of June 2018, identified as case A in Accra (5.6°N and 0.17°W), and the 28th of June 2018, identified as case B in Kumasi (6.72°N and 1.6°W), as shown in Figure 1, during the peak rainy season (June) of southern sector of Ghana have been investigated focusing on the meteorological conditions that led to the heavy rainfall.

2.2. Data and Methodology. Datasets used in this study for the evaluation were in situ rainfall data (45 stations), Global Satellite Mapping of Precipitation (GSMaP), Ghana Meteorological Agency (GMet), GMet Weather Research and Forecasting (WRF) model output, and Meteo France Arpege 0.5 mean sea level pressure (MSLP), a product from the Meteosat Second Generation (MSG) Preparation for Use of MSG in Africa (PUMA) project. The rainfall datasets are daily cumulative rainfall amounts recorded at the various stations measured with rain

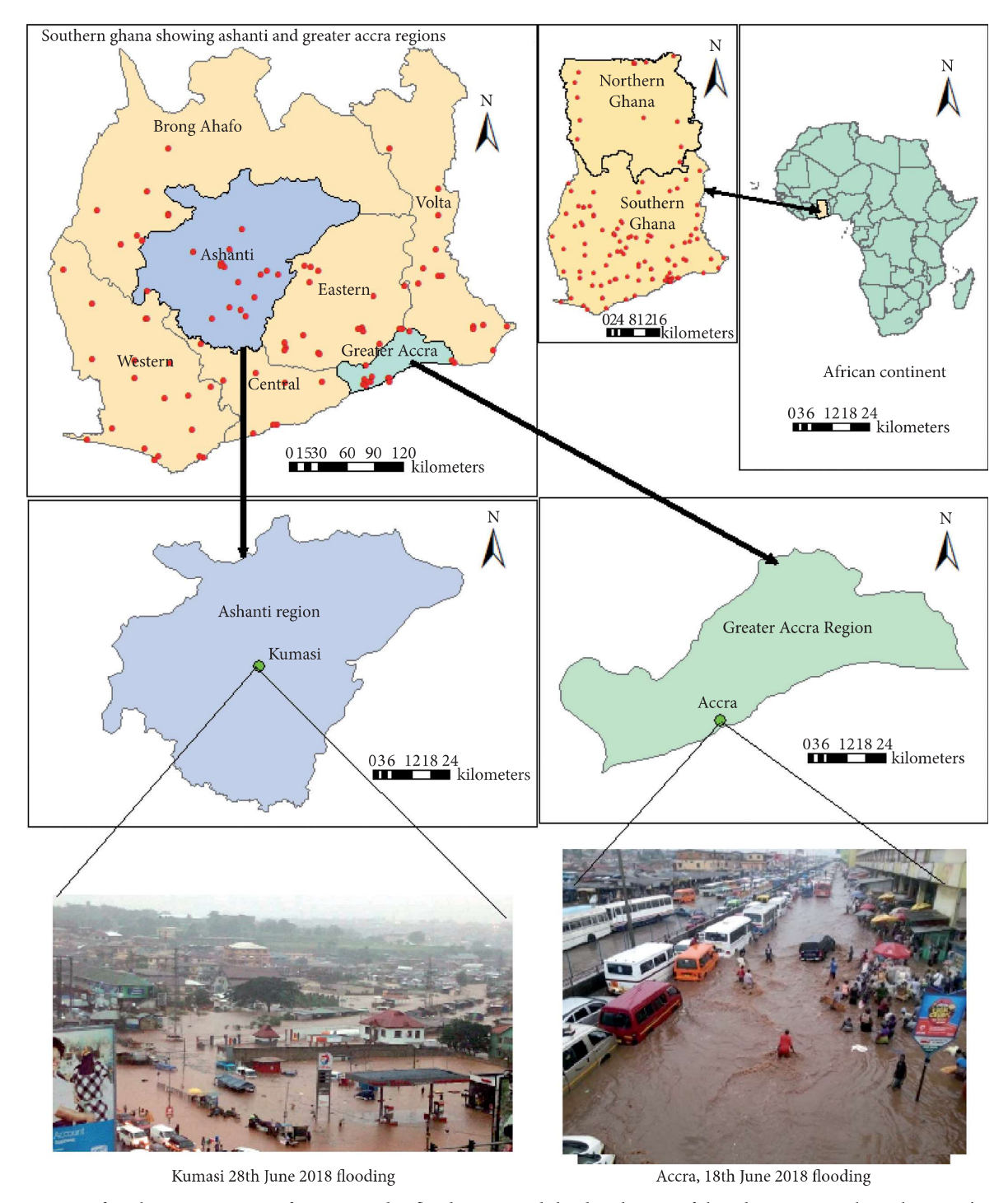


FIGURE 1: Map of study area. Location of cases A and B flood events and the distribution of the Ghana Meteorological Agency's weather observation stations (red dots).

gauges. Sources of error that may affect rainfall measurement or data according to Mensah et al. [37] include evaporation, wetting, wind induced errors, and instrument reading errors on the part of observers. In order to avoid some of these errors, wind shielded rain gauges are used by GMet.

To track the evolution of the rainfall events for this study, the hourly GSMaP images (Figures 2 and 3) were used to

track the genesis, development, dissipation, and the active spots of the thunderstorms as they propagated zonally for cases A and B, respectively. For case A, the thunderstorm affected the coast of Ghana and lasted for about 17 hours before dissipating.

At 18 UTC, the slow-moving thunderstorm hit the eastern coast of Ghana (Figure 2(d)) and after three hours it had reached Accra as it intensified (Figure 2(e)). The storm

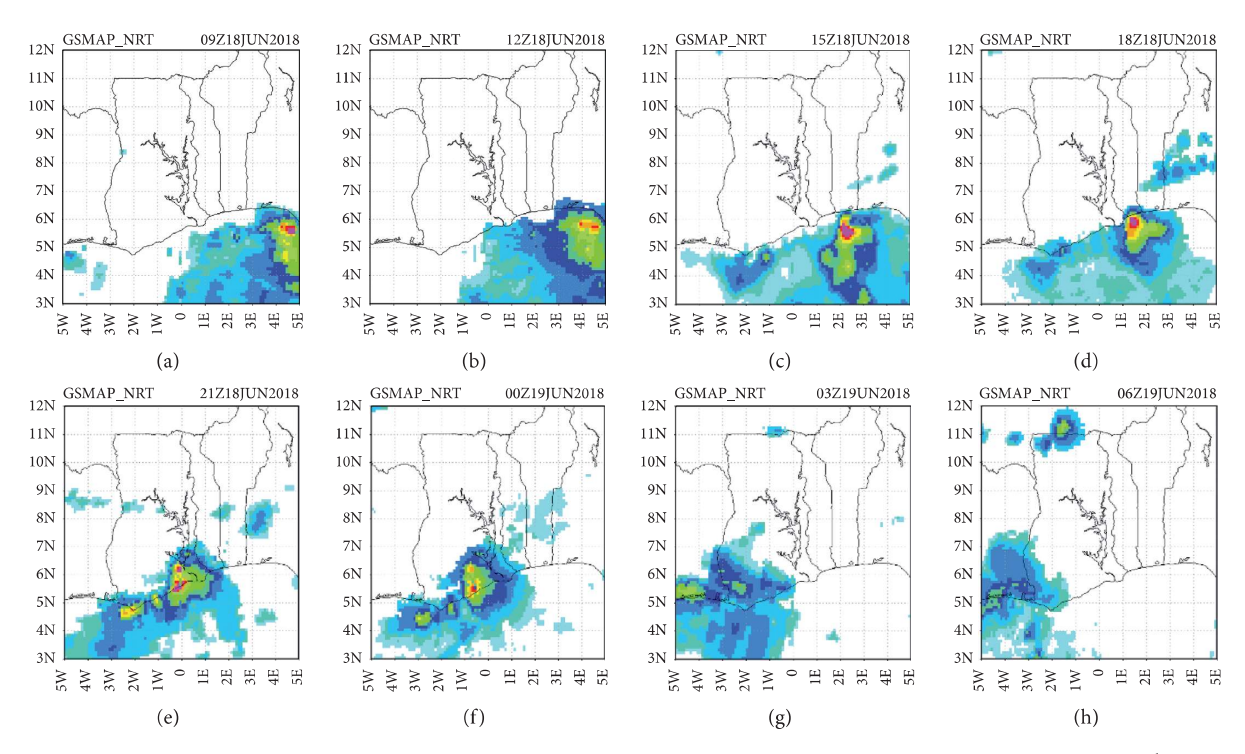


FIGURE 2: GSMaP satellite products. Three hourly precipitation intervals from 09 UTC of the 18th of June to 06 UTC of the 19th of June 2018 for case A.

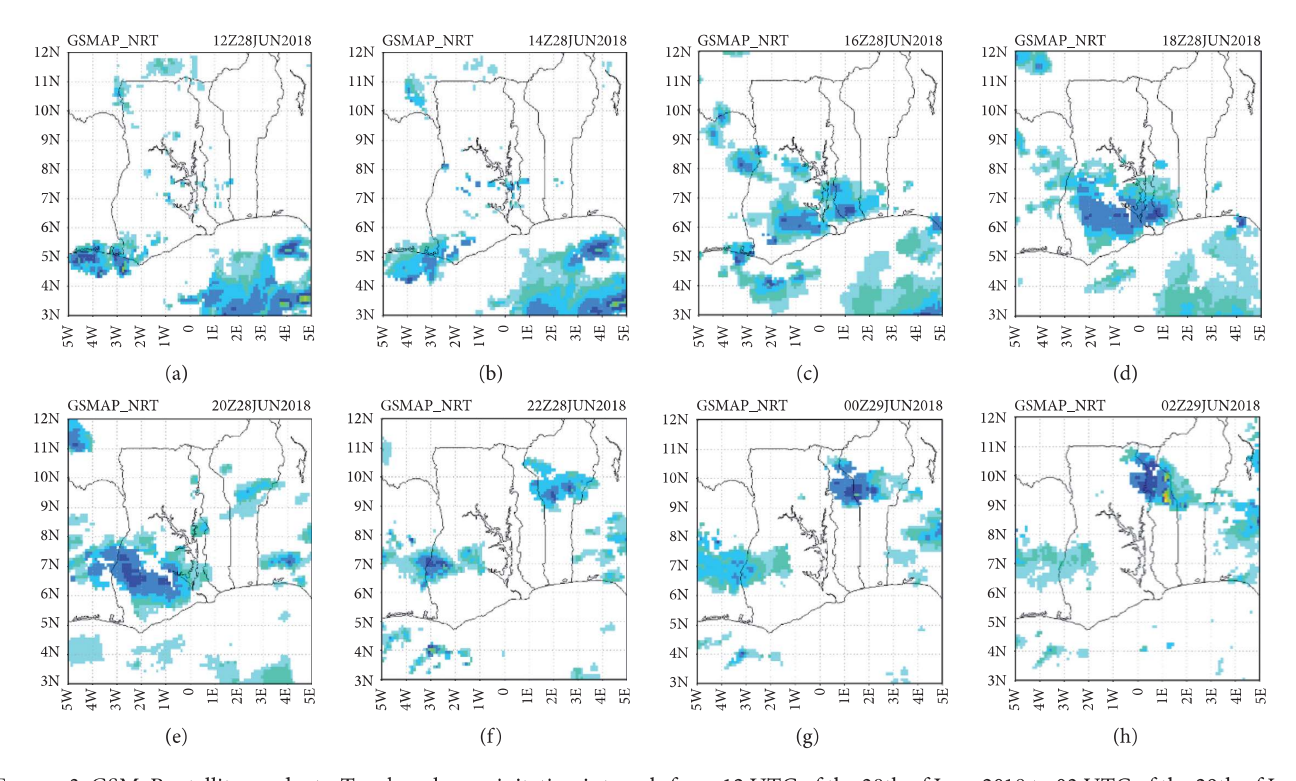


FIGURE 3: GSMaP satellite products. Two hourly precipitation intervals from 12 UTC of the 28th of June 2018 to 02 UTC of the 29th of June 2018 for case B.

finally moved westwards from Accra after 06 UTC on the 19th of June, lasting for about 9 hours. As the storm moved slowly westwards across the eastern coast, the cloud top temperature was observed to change from about -75°C to

about -90°C (estimated using the Meteorological Product Extraction Facility (MPEF) from the Synergie), an indication of its intensification which lasted for about 8 hours (Figure 2(e)). Rainfall amounts recorded over some stations

in the east coast were 124.8 mm, 90.1 mm, and 109.0 mm at Saltpond, Accra, and Pokuase, respectively.

For the flooding event in Kumasi, a localized convective cell started developing within the country in the afternoon (Figure 3(c)). It intensified over the middle sector and produced heavy rains lasting for a period of about 8 hours before dissipating at approximately 02 UTC on the 29th of June (Figure 3(f)). Kumasi had the highest rainfall of 114.6 mm and Kwadaso, a suburb of Kumasi, had 81.0 mm. The spatial distributions of rainfall for the two cases are shown in Figure 4.

The WRF model product used in this study includes the wind, relative humidity (RH), and the skew-T for the second domain. The atmospheric forcing data used for the initial and lateral boundary condition of the model was the global forecasting system (GFS), which was dynamically down-scaled for two domains with resolutions of 27 km and 9 km, respectively, as illustrated in Figure 5. The model's configuration setup uses Betts–Miller–Janjic's [38] convective parameterization scheme for both domains with 49 vertical levels. The inner domain model products were used.

3. Results and Discussion

3.1. Rainfall Time Series Analysis. The long-term (1981–2010) monthly mean rainfall amounts (MMR) for stations along the coast and middle sectors were analyzed (Figure 6) and all showed bimodal rainfall pattern. However, the major differences between the two sectors are land cover and topography of the area, which have an influence on the rainfall pattern [37]. Kumasi (286.3 m above MSL) in the middle sector where case B flood occurred has more vegetation cover than Accra (67.7 m above MSL) where case A flood occurred. It was observed that all the stations along the coast and the middle sector recorded higher rainfall amount during the peak of the major season in June than that of the minor season in October except Akim Oda and Wenchi which recorded 200 mm and 170 mm, respectively, for the major season as compared to 220 mm and 200 mm for minor peak, respectively.

This anomaly could be attributed to seasonal to subseasonal variations. Axim (37.8 m above MSL), the wettest rainfall station in Ghana along the western coast, recorded the highest MMR of 500 mm and 230 mm for peak of the major and minor seasons, respectively. This could be associated with the orientation of its coastline and the vegetation cover. Accra and Kumasi which are the main focus of this study recorded MMR of 180 mm and 215 mm during the peak of the major season, while the peak of the minor season recorded 60 mm and 170 mm, respectively.

The time series of the ADMR variability (1961–2017) over Accra has a positive slope of 0.45 and Kumasi has a negative slope of –0.07 as shown in Figure 7. The top three highest ADMR amounts ever recorded in Accra are 243.9 mm, 212.3 mm, and 175.3 mm which occurred on the 3rd of July 1995, 3rd of June 2015, and 22nd of June 1973, respectively, while Kumasi recorded 167.9 mm, 145.8 mm, and 125.2 mm on the 21st of July 1966, 13th of June 1986, and 5th of May 1997, respectively. It is interesting to note that

Accra's first three highest ADMR values were higher than those of Kumasi.

It is worth noting that these records occurred at the peak of the West African Monsoon season over the respective stations. This can be attributed to its location along the coast where rich moisture from the Gulf of Guinea fuels thunderstorms development as well as land and sea surface temperature variations producing heavy rainfall [39]. The frequency of these extreme rainfall events using the 95th percentile threshold with a value of 45.10 mm and 42.16 mm over the two areas shows a positive slope (Figure 8) of 0.02 (Kumasi) and a negative slope of -0.02 (Accra). This indicates that the chance of extreme rainfall over Kumasi is increasing, while that of Accra is decreasing based on the respective threshold values.

Further analysis on the ADMR distribution and frequency over Accra and Kumasi using the normal distribution shows that 68% of the area of the normal distribution for Accra was between 53.03 mm and 136.81 mm of rainfall, which implies that most of the rainfall events occurred within the 1st z-score distribution value, while 95% of the area of the normal distribution was found between 11.14 mm and 178.70 mm of the 2nd z-score distribution value. The mean ADMR over Accra is 94.92 mm with a standard deviation of 14.89, as shown in Figure 9. The rainfall distribution for Kumasi shows that 68% of the area of normal distribution was between 64.37 mm and 108.87 mm, which implies that most rainfalls were within the 1st z-score distribution value. The 95% of the area of normal distribution ranged from 42.12 mm to 131.12 mm, which satisfied the 2nd z-score distribution value. The mean ADMR is 86.62 mm with a standard deviation of 22.25, as shown in Figure 9(c), where N is 57, representing the total number of years of data used. Table 1 summarizes the 1st and 2nd z-score ADMR values over Accra and Kumasi.

3.2. Charts Analysis. This section reviews the atmospheric dynamics and associated physical mechanisms responsible for the flooding incidents that occurred on those fateful days within southern Ghana. The 12 UTC and 18 UTC prognostic charts used for the 18th and 28th of June 2018 forecast preparation were retrieved and examined. Generally, the quasi-static high pressure systems and their consequent effect on the ITB determine the prevailing weather within the West Africa subregion. During the rainy season, the country is influenced by the maritime air mass due to the intensification of northward ridging of the St. Helena high-pressure system, which drives moisture into the subregion, while the Azores high-pressure system weakens.

3.2.1. Mean Sea Level Pressure (MSLP). From the Meteosat Second Generation (MSG) Preparation for Use of MSG in Africa (PUMA) station, MSLP charts at 12 UTC for case A showed that St. Helena had a center value of 1027 hPa, while Azores was 1030 hPa with the equatorial trough (ET) extended zonally to the east of the continent as shown in

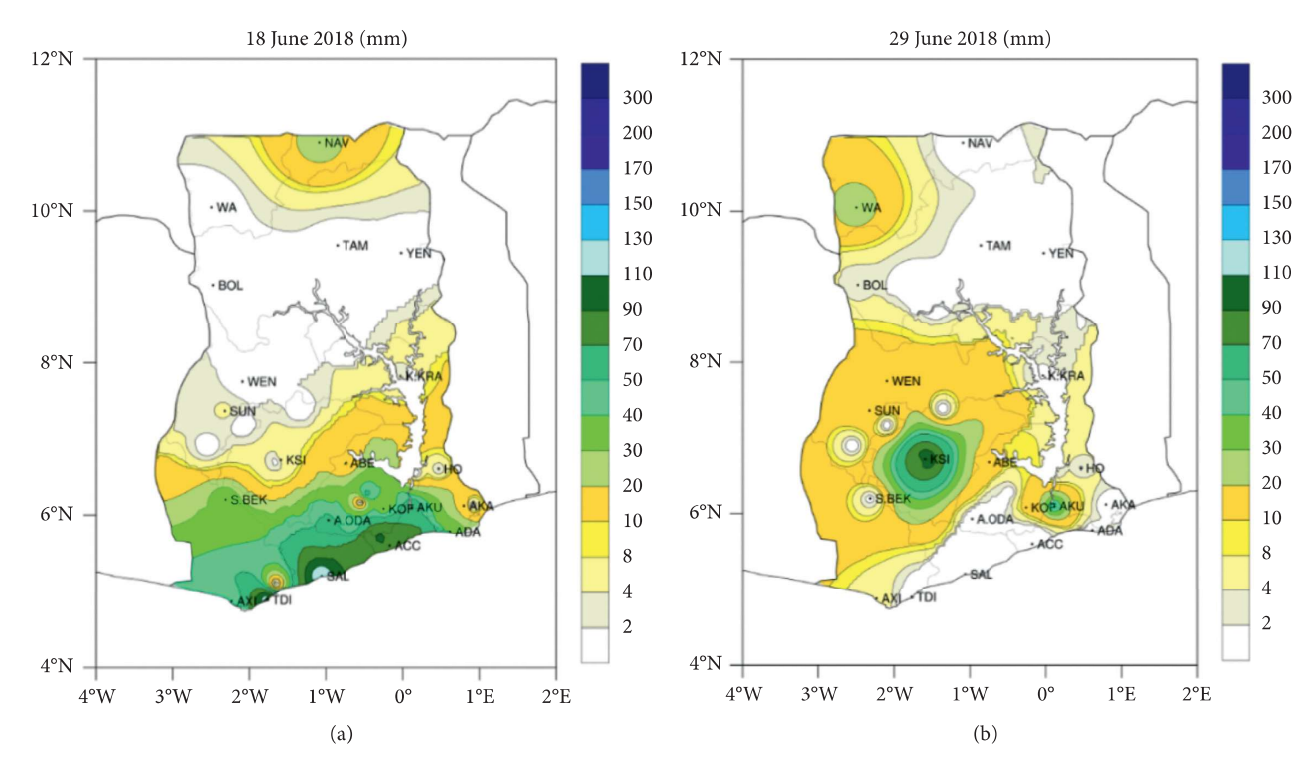


FIGURE 4: Distribution of rainfall (mm). (a) Case A and (b) case B.

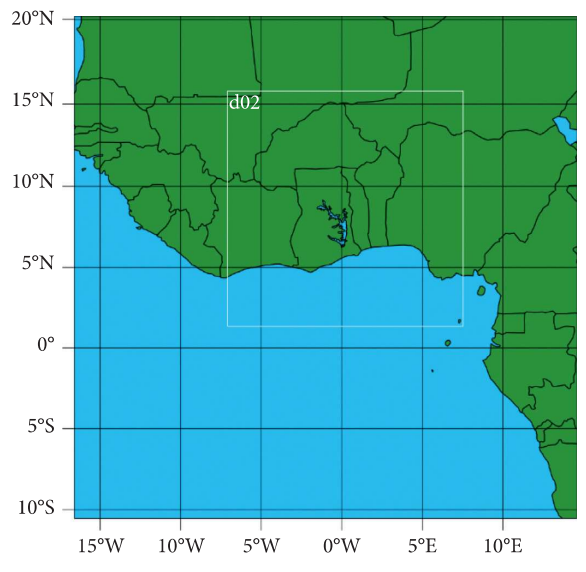


FIGURE 5: Two domain configurations for GMET's WRF model. Resolutions of 27 km and 9 km (white cell), respectively.

Figure 10(a). The country was between the pressures of 1012 hPa to the north and 1016 hPa to the south. By 18 UTC, the St. Helena and Azores center pressures dropped to 1025 hPa and 1029 hPa, respectively, with zonal and meridional expansion of the ET where the country's pressure was between 1015 hPa and 1010 hPa.

Low pressure centers of 1005 hPa and 999 hPa were observed, respectively, between the borders of Mauritania and Mali as well as central Chad as shown from Figure 10(b).

The Azores and St. Helena high-pressure centers for case B were 1022 hPa and 1027 hPa, respectively, as at 12 UTC. The ET extended covering most parts of Niger (excluding the southern fringes and whole of Burkina Faso), northern half of Mali, and eastern Mauritania through to southern half of Algeria. The isobar over Ghana ranged between 1012 hPa to the north and 1014 hPa to the south (Figure 11(a)). At 18 UTC, there was a 2 hPa drop in the core values of the Saint Helena high-pressure system, while that of Azores was maintained. This

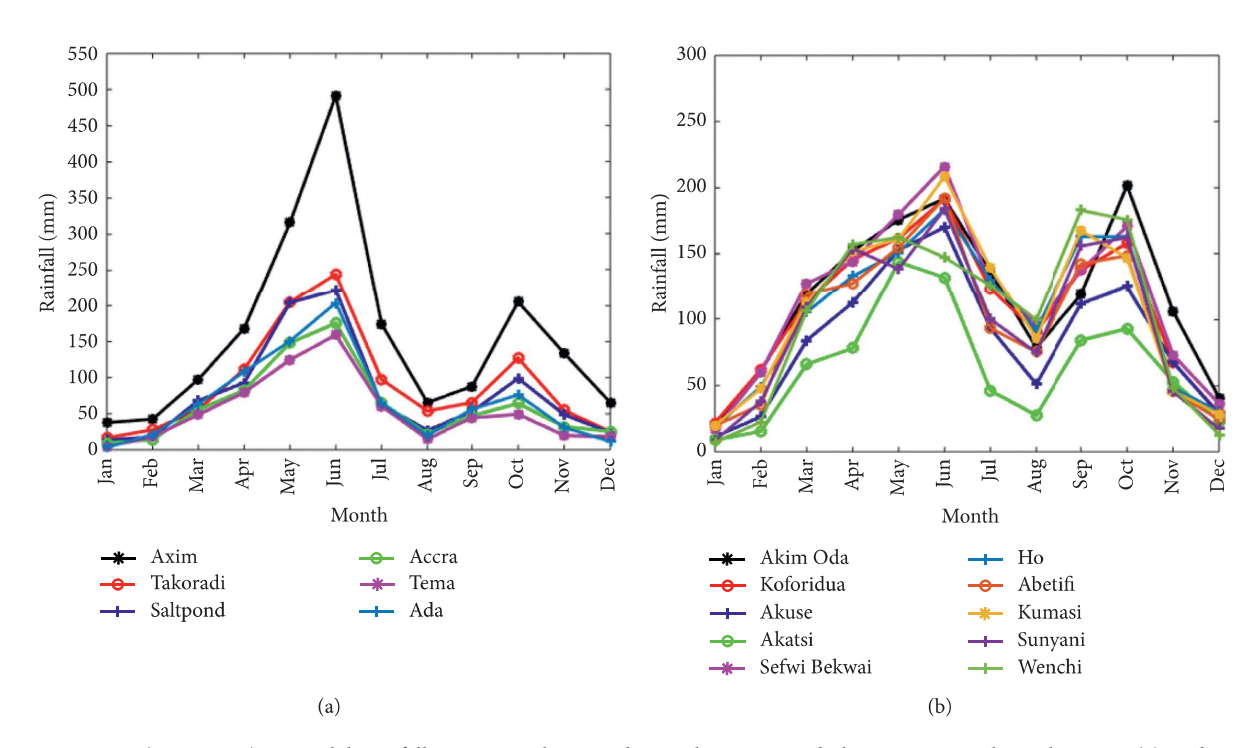


FIGURE 6: MMR (1981–2010). Bimodal rainfall pattern within Southern Ghana: six and eleven stations along the coast (a) and over the middle sector (b), respectively.

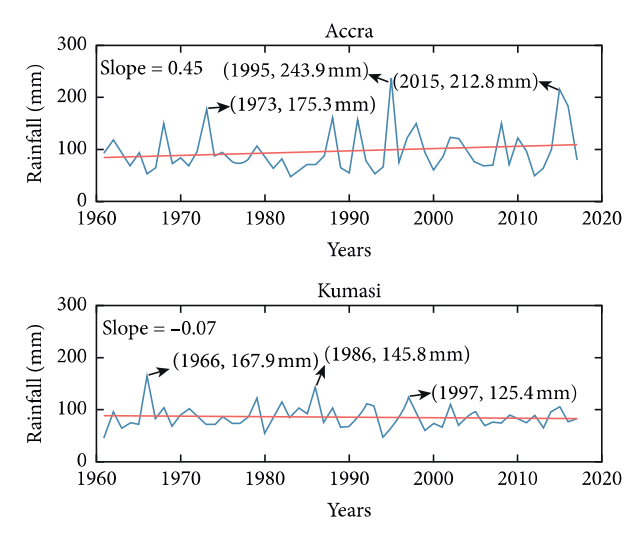


FIGURE 7: ADMR (1961-2017). Rainfall variability over Accra and Kumasi.

condition triggered both zonal and meridional expansions of the ET with the lower portions stretching and covering north (Nigeria, Benin, Togo, Ghana, Ivory Coast, Guinea, and Senegal). The isobar over Ghana ranged between 1010 hPa to the north and 1012 hPa to the south (Figure 11(b)).

3.2.2. Wind and Moisture. The GMet WRF model was able to forecast the moisture laden winds at the 850 hPa level (Figures 12(a) and 12(d)) with speed ranging between 10 knots (5 ms⁻¹) and 20 knots (10 ms⁻¹) at 12 UTC and then it increased to 25 knots (13 ms⁻¹) by 18 UTC for the coastal

sector. The Africa Easterly Jet (AEJ) at 700 hPa level (steering level) which had southerly components was weak (i.e., speed between 5knots (2.5 ms⁻¹) and 15 knots (7.5 ms⁻¹)); hence, it influenced the slow propagation of the storm as marked by the broken red oval shape in Figures 12(b) and 12(e).

In case B, significant amount of moisture (RH > 80%) was also observed at the 850 hPa and the 700 hPa levels, which reflects the extent of moisture depth within the atmosphere. The south westerly winds filled a cyclonic vortex with speed between 5 and 10 kts (3–5 ms⁻¹) located north of

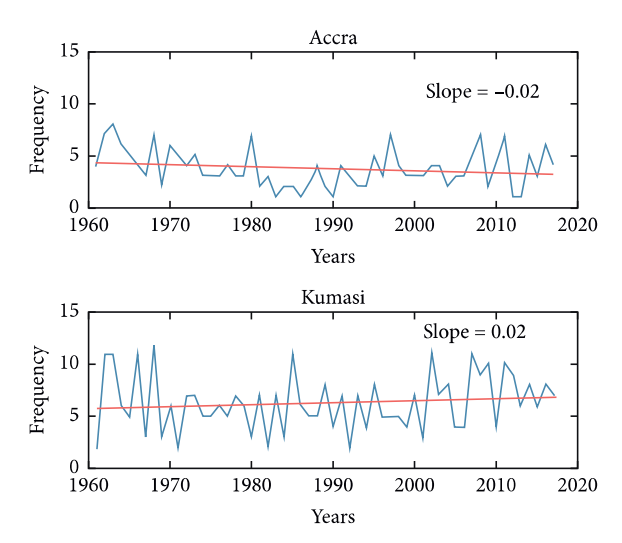


FIGURE 8: Annual rainfall frequency (ARF). Accra and Kumasi ARF based on the 95th percentile thresholds of 45.10 and 42.16 mm, respectively.

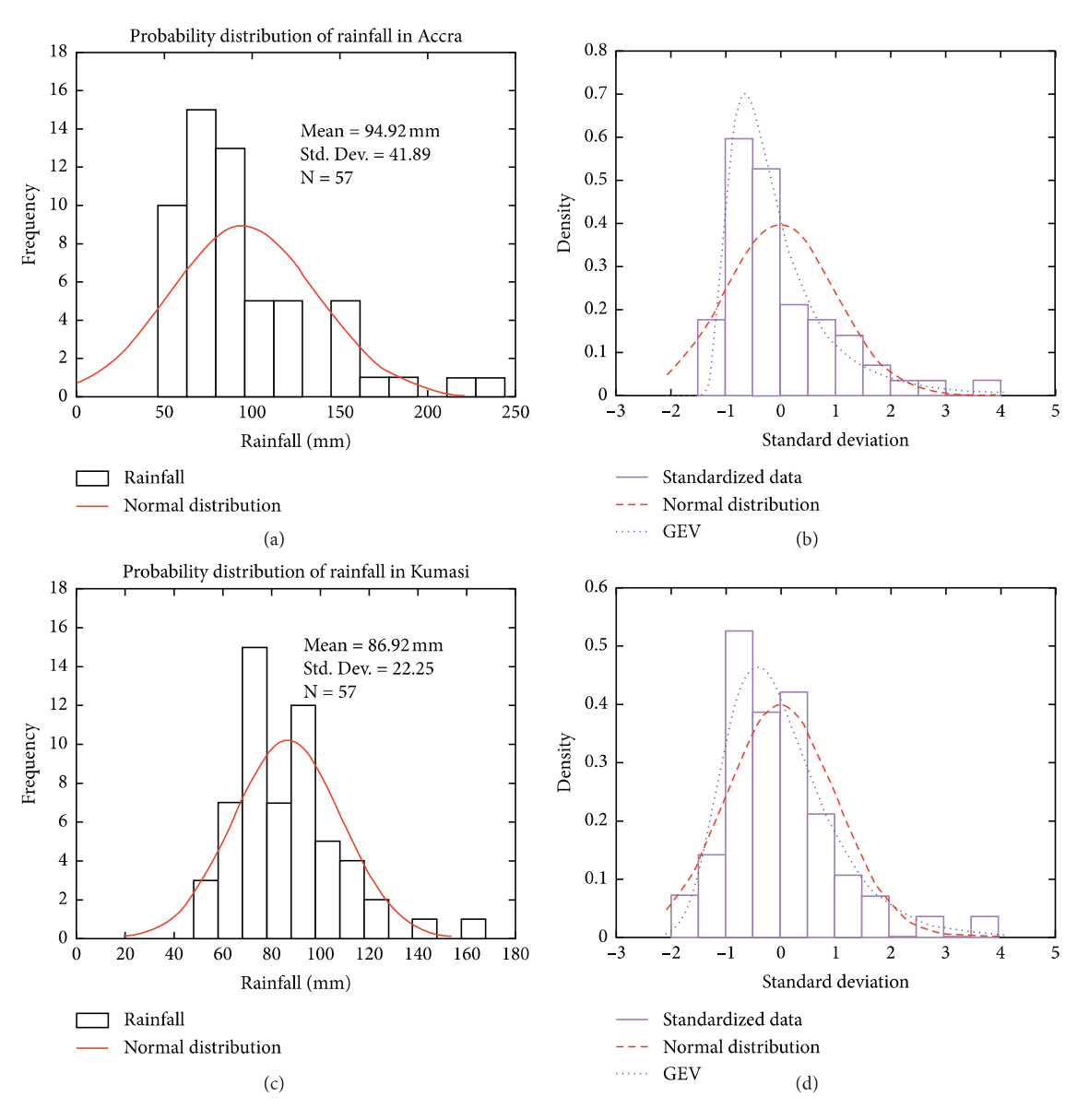


FIGURE 9: Normal and standardized rainfall distribution. Plots (a) and (b) and (c) and (d) for cases A and B, respectively.

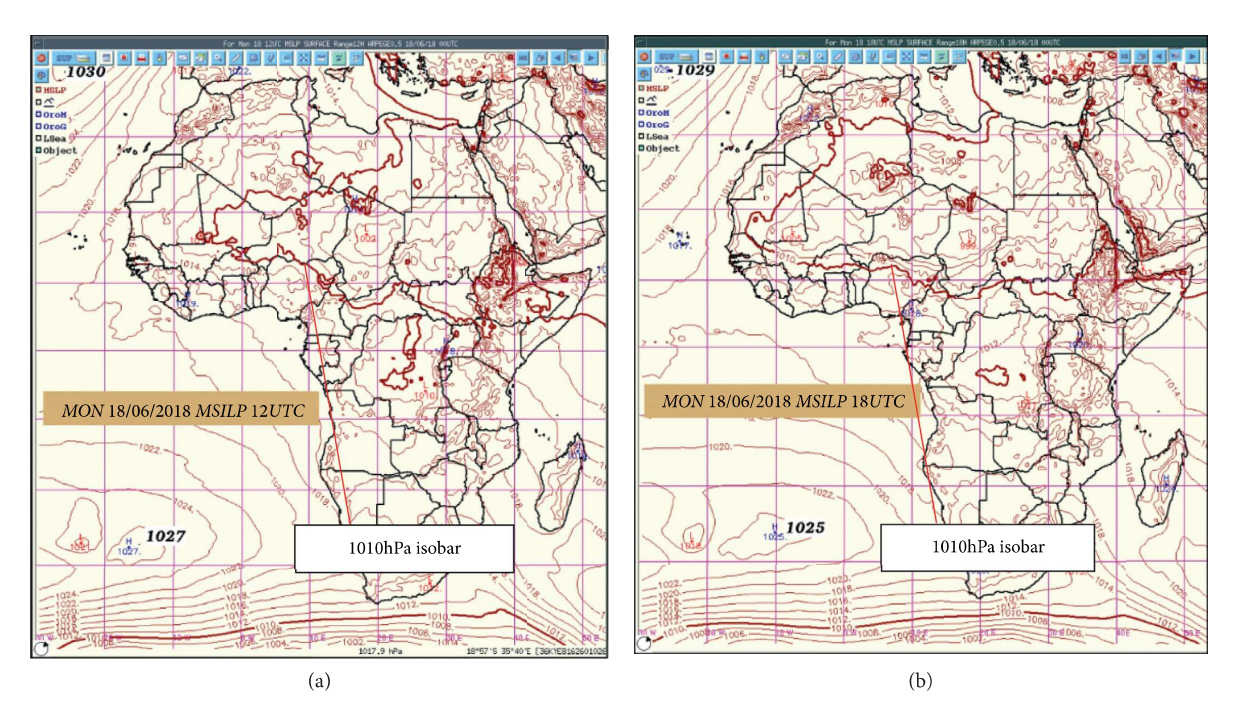


FIGURE 10: Meteo France Arpege 0.5 MSLP charts. (a) 12 UTC and (b) 18 UTC for case A.

Table 1: The 68% and 95% of the area of normal distribution for cases A and B from annual daily maximum rainfall (mm), respectively.

Event	68% area of no	rmal distribution	95% area of normal distribution		
	$\mu - \varepsilon$	$\mu + \sigma$	μ – 2σ	$M + 2\sigma$	
Case A	53.03	136.81	11.14	178.7	
Case B	64.37	108.87	42.12	131.12	

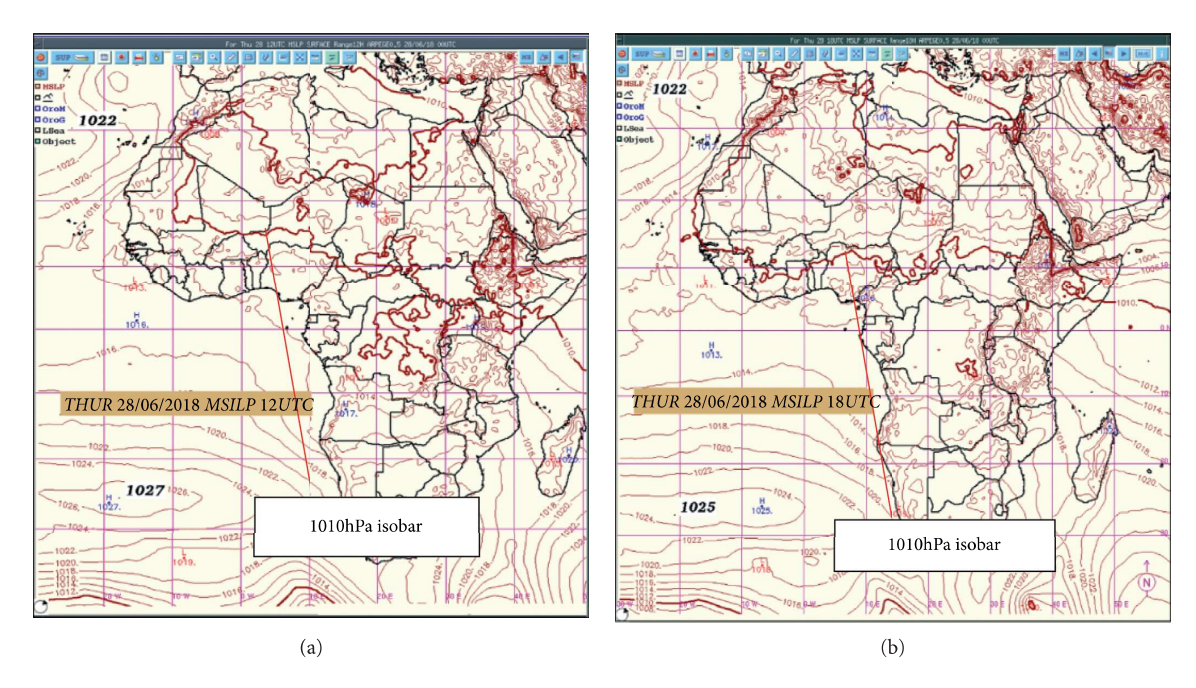


FIGURE 11: Meteo France Arpege 0.5 MSLP charts. (a) 12 UTC and (b) 18 UTC for case B.

Benin at 12 UTC (Figure 13(a)). At 18 UTC (Figure 14(b)), the speed increased to 15 kts (8 ms⁻¹), especially for the coast. There were direct AEJ at 700 hPa with speeds between 15 and

25 kts (Figures 12(b), 12(e), and 13(b)). The upper level jet (200 hPa) was direct easterlies with speed around 35 kts. The convective activities observed in Figure 3 were a result

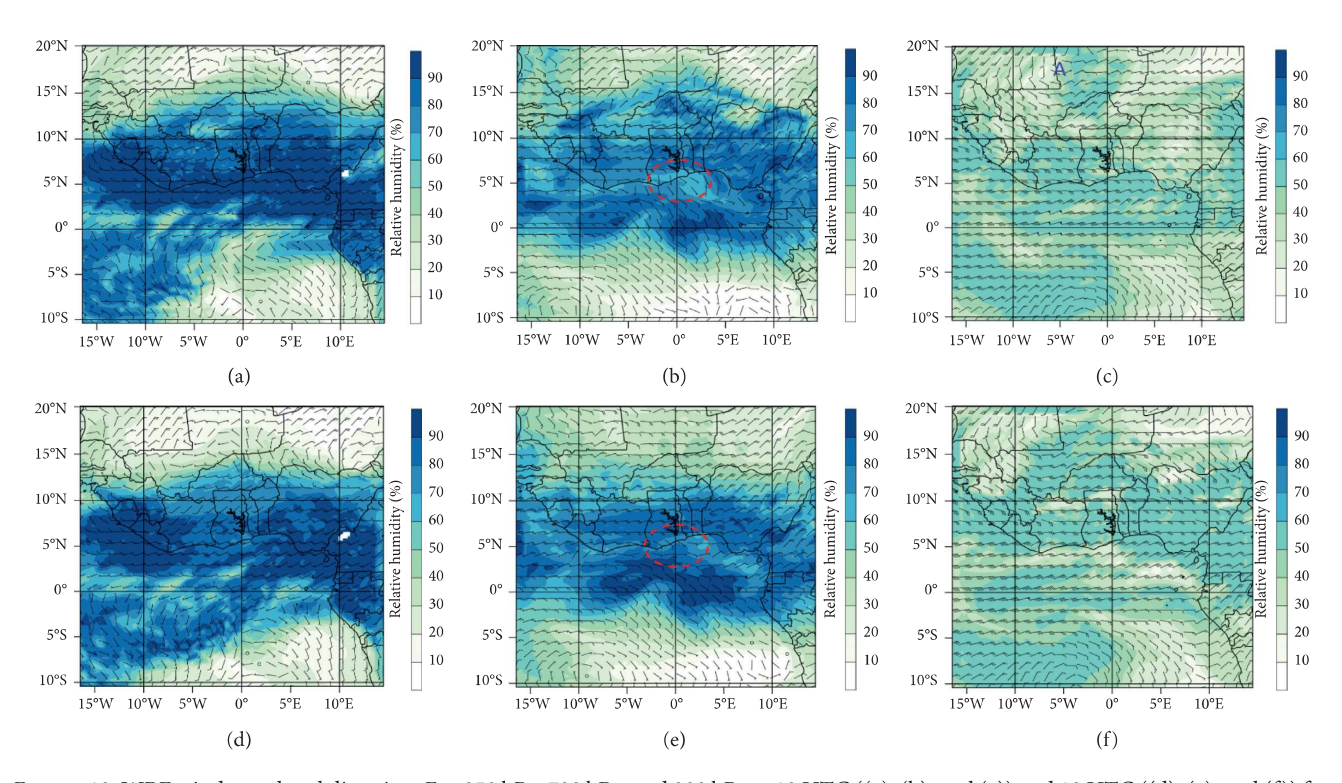


FIGURE 12: WRF wind speed and direction. For 850 hPa, 700 hPa, and 200 hPa at 12 UTC ((a), (b), and (c)) and 18 UTC ((d), (e), and (f)) for case A.

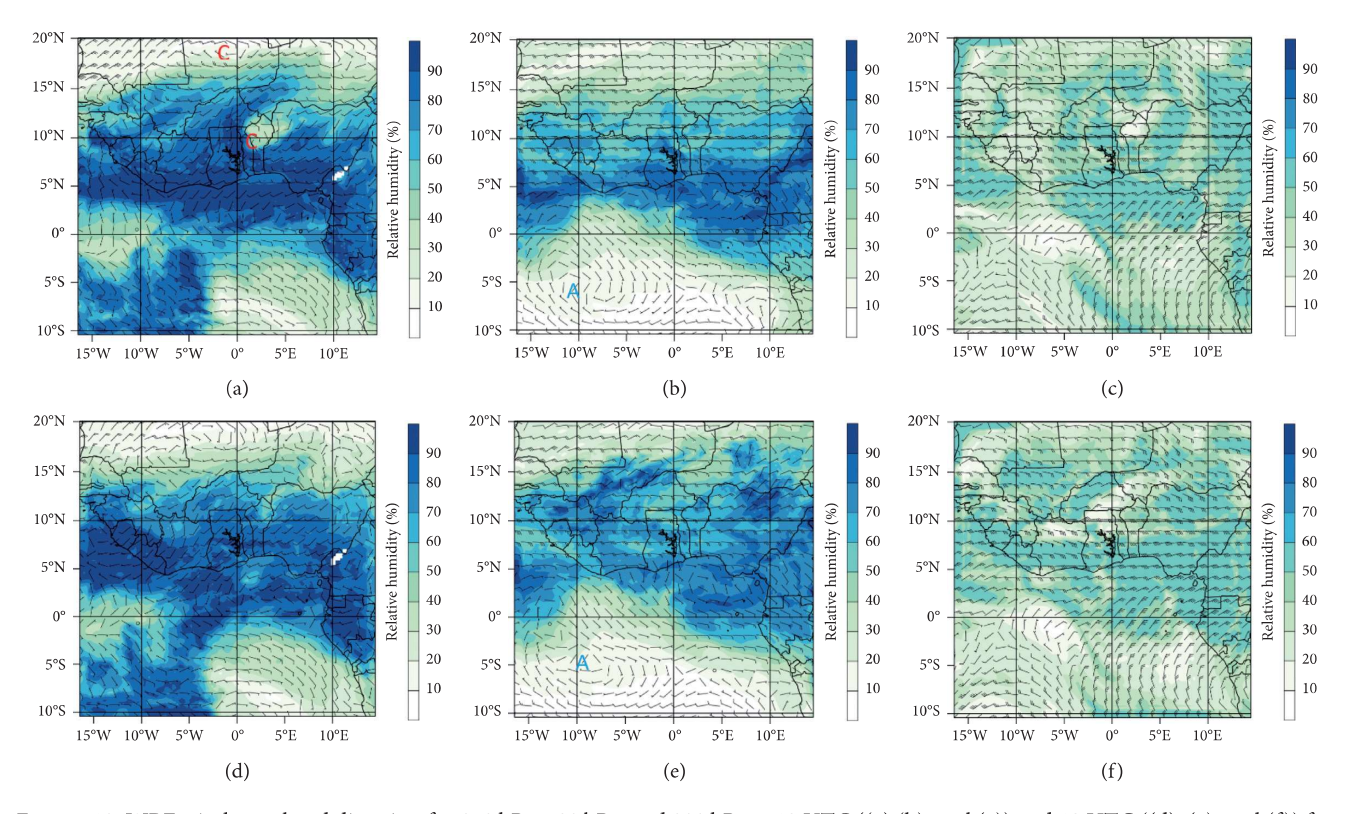


FIGURE 13: WRF wind speed and direction for 850 hPa, 700 hPa, and 200 hPa at 12 UTC ((a) (b), and (c)) and 18 UTC ((d), (e), and (f)) for case B.

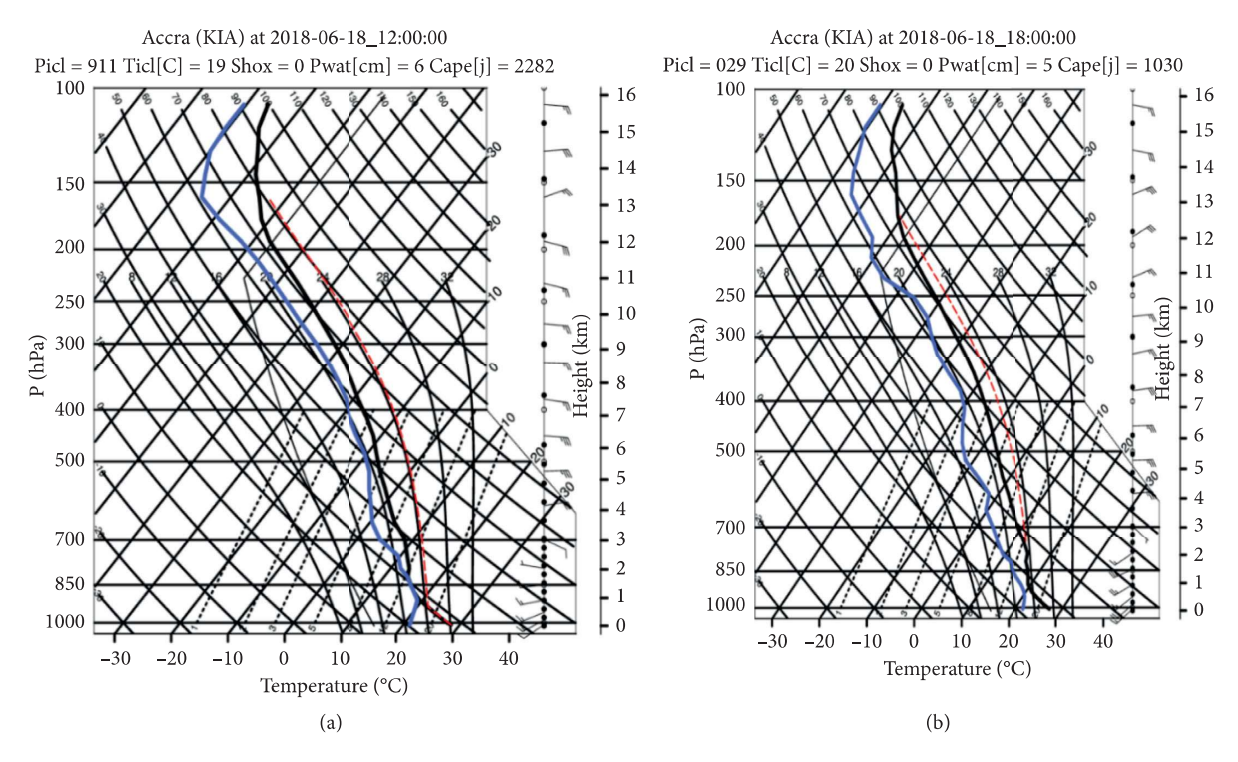


FIGURE 14: WRF skew-T diagram showing atmospheric dynamics for case A (a) at 12 UTC and (b) at 18 UTC.

of local meteorological features where orographic forcing and vegetation cover as in Kumasi (above 286.3 m) have been established for many years by both research and local forecasters experience [33] to have significant influence on convective initiations. The main cause of this triggering is the diurnal heating over higher elevations coupled with the moisture within the atmosphere. These characteristics contributed to the development and spread of the convective cells, resulting in the heavy rainfall experienced in Kumasi.

Meanwhile, the African Easterly Wave (AEW) troughed along Togo-Benin coast and then extended to the coast of Ghana and deepened by 18 UTC (Figures 12(b) and 12(e)). From Figures 12(c) and 12(f), an anticyclonic vortex observed at 200 hPa level, located close to the western border of Mali, ridged over the subregion with weak Tropical Easterlies Jets (TEJ). These conditions ahead of the system supported the westward propagation of the storm, thereby playing significant role in its kinetics. It was observed that an appreciable amount of moisture (RH) above 80% at 850 hPa and the 700 hPa was within the atmosphere indicating saturation for storm formation at the 850 hPa levels (Figure 12). Moreover, tidal waves on that day were high, which were aided by low surface pressure over the coastal area for the entire period of the event. The convective available potential energy (CAPE) in the WRF skew-T (Figures 14 and 15) showed enhanced instability in the atmosphere for convective processes. It has been established that low level convergence (i.e., at 925 hPa pressure level) of moisture and upper level divergence are good indicators for large scale precipitation [40, 41]. However, localized moisture convergence and mesoscale lifting could also produce a

water-saturated cloud layer from which deep moist convection subsequently evolves [42].

The dew point (blue lines) and the temperature (red lines) profiles showed high levels of humidity (>70%) and temperature profiles of the atmosphere for more cloud formations especially between 925 hPa and 850 hPa where the convective condensation level (CCL) can be estimated. This is in agreement with the relative humidity estimates seen on the WRF output in Figures 12 and 13. The convective available potential energy (CAPE) at 12 UTC for cases A and B was 2282 J/kg and 2439 J/kg, respectively, while at 18 UTC it dropped to 1039 J/kg and 1997 J/kg, respectively. Tajbakhsh et al. [43] used the Miller checklist to categorize the severity of thunderstorms. From this checklist, it is observed that most of the parameters available to determine the strength in both cases implied that the storms were weak (Table 2).

Comparing the daily rainfall amounts recorded for cases A and B, they were not exceptional and not even close to the 3rd highest of the ADMR amounts which caused the floods and resulted in casualties and damage of properties. As climate varies geographically, the definition of extreme weather thresholds will also vary. This was observed for the 95th percentile threshold values over Accra and Kumasi. For best practices globally, [44] established a tasked team on the definition of extreme weather and climate events which classified heavy rainfall threshold greater than 50 mm (>50 mm/24 hr.) per day. It was observed that most rainfalls for the flood events fell below the threshold over Accra and Kumasi (Figure 16).

Possible reasons for these flooding cases can be related to nonmeteorological factors which included poor drainage

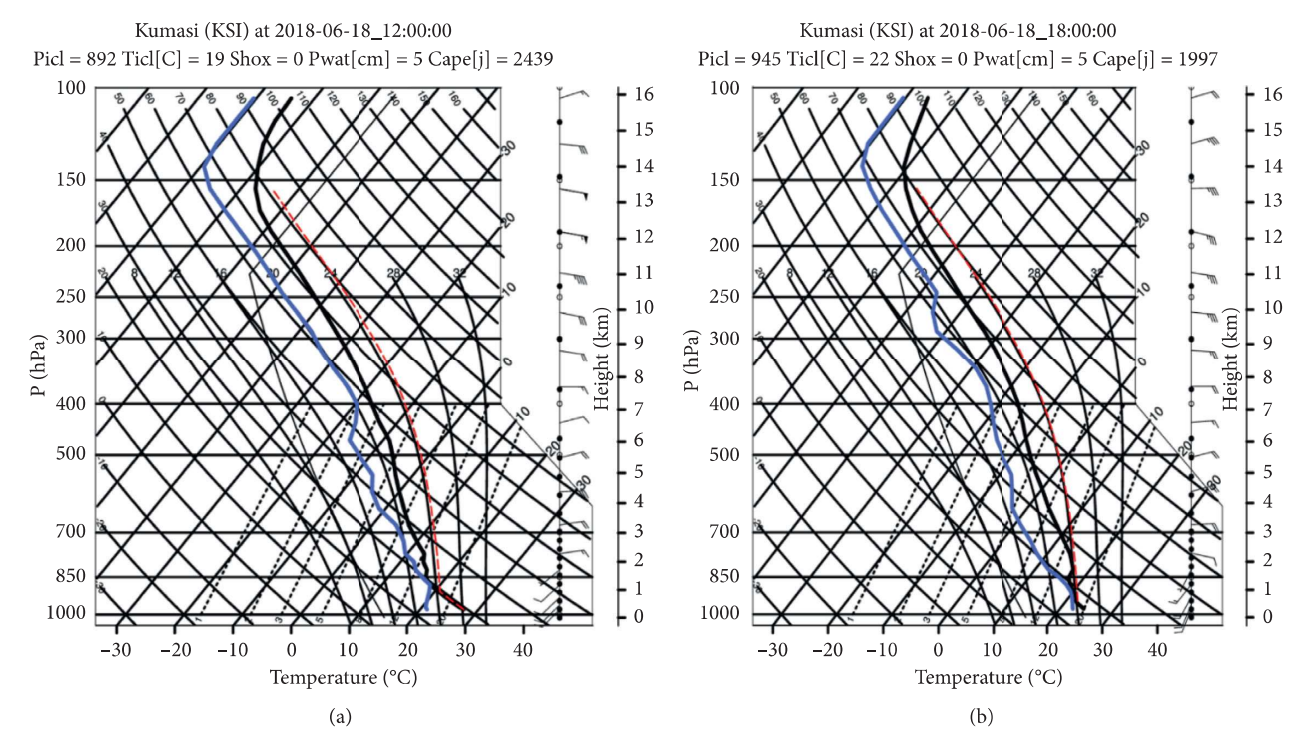


FIGURE 15: WRF skew-T diagram showing atmospheric dynamics for case B (a) at 12 UTC and (b) at 18 UTC.

Table 2: Miller checklist of some selected parameters for severe weather adopted from Tajbakhsh et al. [43].

Damanastan	Case A		Case B		Miller checklist		
Parameter	12 UTC	18 UTC	12 UTC	18 UTC	Weak	Moderate	Strong
Surface pressure	1015 hPa	1014 hPa	1014 hPa	1012 hPa	>1010 hPa	1010-1005 hPa	<1005 hPa
Dew point	22°C	23°C	21°C	22°C	<2.8°C	12.8-17.8°C	18.3°C
CAPÉ	2282 J/kg	1039 J/kg	2439 J/kg	1997J/kg	800-1500 J/kg	1500-2500 J/kg	>2500 J/kg
Mean RH	90%	70%	90%	80%	70-80% or 40-50%	50-70%	50-70%
850-500 hPa wind shear	5-35 kts	5-35 kts	5-25 kts	5-20 kts	15-25 kts	26-35 kts	>35 kts

systems, building on water ways, improper disposal of refuse, limited roof-top rain harvesting in urban area, land cover change, less lawn, and limited tree planting. In their work also confirmed that intensive and unplanned human settlements in flood-prone areas played a major role in increasing flood risk in Africa as observed in most parts of Accra (e.g., Avenor and Kaneshie) and Kumasi (e.g., Buokrom and Anloga junction) [6].

Generally, the month of June is the peak of the major rainy season over southern Ghana. Consecutive days of rainfall over the high grounds and the inland areas were continually drained off to the sea. Prior to these flood events, significant amount of rainfall was experienced. For case B, the city being a coastal town and at comparatively low altitude receives run-offs from the high grounds and discharges off to the sea.

Accra is one of the most densely populated cities in the country, with high rural-urban migration resulting in unplanned settlements. The waste generated mostly ends up in the drains and is washed into water bodies which

ultimately end up in the sea. City dwellers occupy riparian zones and wet-lands leading to flood initiation when moderate rains occur. It is a great challenge for city planners to control and regulate infrastructural activities in the area. These play a greater role in causing flood events with moderate rainfall.

4. Conclusion

This study investigated the meteorological dynamics for the heavy rainfall that resulted in flood over Kumasi and Accra. Qualitative analysis was done using graphical representation of the thunderstorm propagation from GSMaP and global and regional model outputs results. In order to establish the uniqueness of the event as a result of its damage, a comparative analysis was done with historical flood occurrence. The results from meteorological analysis indicate that MSLP was low with significant moisture influx for thunderstorm system growth and development. It was observed that the thunderstorm thrived under weak synoptic features, even

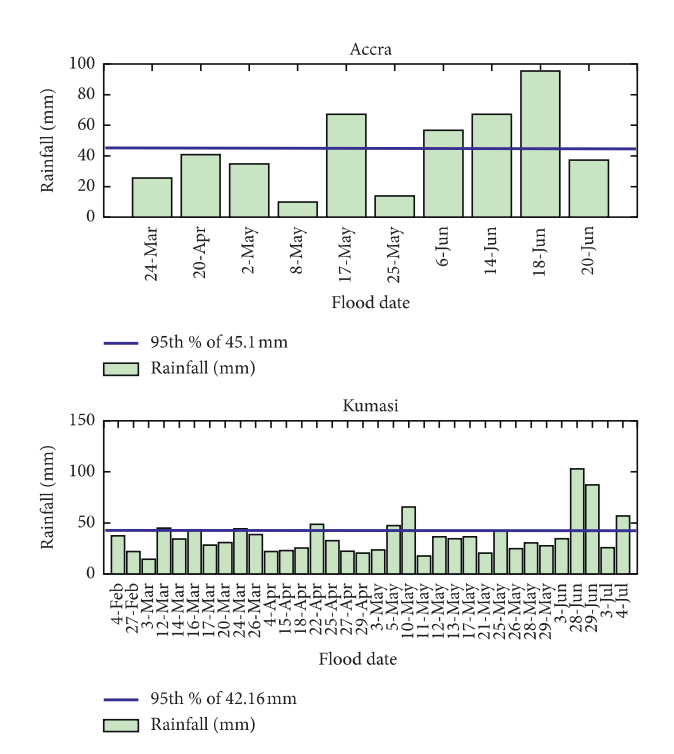


FIGURE 16: Accra and Kumasi 95th percentile threshold. This shows most flood events below the threshold.

though the moisture was enough for its survival. This led to its slower movement and subsequent stagnation. Moreover, it was also observed that the weak AEJ (at 12 UTC and 18 UTC) contributed to its weak propagation. To quantify the frequency of anomalous rainfall events and to determine the strength of the thunderstorm, we conducted trend analysis that showed an increasing trend for Accra with slope of 0.045 and a decreasing trend for Kumasi with slope of –0.07. This also coincides with the less days with heavy rainfall for Accra using the 95th percentile threshold of 45.10 mm and more days with less heavy rainfall for Kumasi using the 95th percentile threshold of 42.16 mm.

Miller checklist for severe weather categorization was used to assess the strength of the thunderstorms for some selected meteorological parameters. From the results as summarized in Table 2, the thunderstorms that led to the heavy rainfalls were weak. This study concludes that the meteorological conditions that aided the formation and propagation of the weather systems that produced the heavy rainfall events resulting in the floods that occurred over the study areas were nonmeteorologically induced. Anthropogenic activities such as buildings on water ways and choked drainage systems were responsible for the floods. Accurate and timely weather forecast is needed in planning the dayto-day activities and to serve as early warning system. This study has shown some of the main synoptic features that produced the heavy rainfall events in Ghana and could serve as a reference for forecasters in Ghana and the West African subregion as far as forecasting heavy rainfall event is concerned. Further studies must be carried out over other areas within the country to determine the 95th threshold for extreme rainfall, especially the flood-prone zones.

Data Availability

The in situ rainfall and WRF data used to support the findings of this study are available from the corresponding author upon request.

Conflicts of Interest

The authors declare that there are no conflicts of interest regarding the publication of this paper.

References

- [1] R. Few, "Flooding, vulnerability and coping strategies: local responses to a global threat," *Progress in Development Studies*, vol. 3, no. 1, pp. 43–58, 2003.
- [2] P. Tschakert, R. Sagoe, G. Ofori-Darko, and S. N. Codjoe, "Floods in the sahel: an analysis of anomalies, memory, and anticipatory learning," *Climatic Change*, vol. 103, no. 3-4, pp. 471–502, 2010.
- [3] D. J. Parker, Floods, Routledge, Abingdon, UK, 2000.
- [4] I. Douglas, K. Alam, M. Maghenda, Y. Mcdonnell, L. McLean, and J. Campbell, "Unjust waters: climate change, flooding and the urban poor in Africa," *Environment and Urbanization*, vol. 20, no. 1, pp. 187–205, 2008.
- [5] BBC, 2007, http://news.bbc.co.uk/1/hi/world/africa/6998651.stm.
- [6] G. D. Baldassarre, A. Montanari, H. Lins, D. Koutsoyiannis, and L. Brandimarte, "Flood fatalities in Africa: from diagnosis to mitigation," *Journal of Geophysical Research Letters*, vol. 37, no. 22, 2010.
- [7] T. G. Amangabara and M. Obenade, "Flood vulnerability assessment of Niger delta states relative to 2012 flood disaster in Nigeria," *American Journal of Environmental Protection*, vol. 3, no. 3, pp. 76–83, 2015.
- [8] N. K. Karley, "Flooding and physical planning in urban areas in west Africa: situational analysis of Accra, Ghana," *Theoretical and Empirical Researches in Urban Management*, vol. 4, no. 13, pp. 25–41, 2009.
- [9] Y. A. Twumasi and R. Asomani-Boateng, "Mapping seasonal hazards for flood management in Accra, Ghana using GIS," in Proceedings of the Geoscience and Remote Sensing Symposium: IGARSS Apos; 02 IEEE International, vol. 5, pp. 2874-2876, Toronto, Canada, February 2002
- [10] D. Rain, R. Engstrom, C. Ludlow, and S. Antos, "Accra Ghana: a city vulnerable to flooding and drought-induced migration: case study prepared for cities and climate change," *Global Report on Human Settlements 2011*, http://www.unhabitat.org/grhs/2011, 2011.
- [11] C. Amoako and E. Frimpong Boamah, "The three-dimensional causes of flooding in Accra, Ghana," *International Journal of Urban Sustainable Development*, vol. 7, no. 1, pp. 109–129, 2015.
- [12] K. Appeaning Addo and M. Adeyemi, "Assessing the impact of sea-level rise on a vulnerable coastal community in Accra, Ghana," *Jàmbá: Journal of Disaster Risk Studies*, vol. 5, no. 1, p. 8, 2013.
- [13] O. Cred, *The Ofda/cred International Disaster Database*, Emdat, Brussels, Belgium, 2009.
- [14] S. Asumadu-Sarkodie, P. A. Owusu, and M. P. C. Jayaweera, "Flood risk management in Ghana: a case study in Accra," *Advances in Applied Science Research*, vol. 6, no. 4, pp. 196–201, 2015.

[15] S. Janicot, G. Caniaux, F. Chauvin et al., "Intraseasonal variability of the west african monsoon," *Atmospheric Science Letters*, vol. 12, no. 1, pp. 58–66, 2011.

- [16] L. Amekudzi, E. Yamba, K. Preko et al., "Variabilities in rainfall onset, cessation and length of rainy season for the various agro-ecological zones of Ghana," *Climate*, vol. 3, no. 2, pp. 416–434, 2015.
- [17] J. B. Omotosho, "Long-range prediction of the onset and end of the rainy season in the west African Sahel," *International Journal of Climatology*, vol. 12, no. 4, pp. 369–382, 1992.
- [18] J. B. Omotosho, A. A. Balogun, and K. Ogunjobi, "Predicting monthly and seasonal rainfall, onset and cessation of the rainy season in west Africa using only surface data," *International Journal of Climatology*, vol. 20, no. 8, pp. 865–880, 2000.
- [19] B. J. Abiodun, Z. D. Adeyewa, P. G. Oguntunde, A. T. Salami, and V. O. Ajayi, "Modeling the impacts of reforestation on future climate in west Africa," *Theoretical and Applied Cli*matology, vol. 110, no. 1-2, pp. 77–96, 2012.
- [20] I. Diallo, M. B. Sylla, F. Giorgi, A. T. Gaye, and M. Camara, "Multimodel GCM-RCM ensemble-based projections of temperature and precipitation over west Africa for the early 21st century," *International Journal of Geophysics*, vol. 2012, Article ID 972896, 19 pages, 2012.
- [21] M. B. Sylla, F. Giorgi, J. S. Pal, P. Gibba, I. Kebe, and M. Nikiema, "Projected changes in the annual cycle of highintensity precipitation events over west Africa for the late twenty-first century," *Journal of Climate*, vol. 28, no. 16, pp. 6475–6488, 2015.
- [22] A. Dosio and H. J. Panitz, "Climate change projections for CORDEX-Africa with COSMO-CLM regional climate mode land differences with the driving global climate models," *Climate Dynamics*, vol. 46, no. 5-6, pp. 1599–1625, 2016.
- [23] N. Kumi and B. J. Abiodun, "Potential impacts of 1.5°C and 2°C global warming on rainfall onset, cessation and length of rainy season in west Africa," *Environmental Research Letters*, vol. 13, no. 5, Article ID 055009, 2018.
- [24] A. Sossa, B. Liebmann, I. Bladé et al., "Statistical connection between the madden-julian oscillation and large daily precipitation events in west Africa," *Journal of Climate*, vol. 30, no. 6, pp. 1999–2010, 2017.
- [25] E. D. Maloney and J. Shaman, "Intraseasonal variability of the west african monsoon and atlantic ITCZ," *Journal of Climate*, vol. 21, no. 12, pp. 2898–2918, 2008.
- [26] S. E. Nicholson, "A revised picture of the structure of the "monsoon" and land ITCZ over west Africa," *Climate Dynamics*, vol. 32, no. 7-8, pp. 1155–1171, 2009.
- [27] M. Diop and D. I. F. Grimes, "Satellite-based rainfall estimation for river flow forecasting in Africa. II: African easterly waves, convection and rainfall," *Hydrological Sciences Journal*, vol. 48, no. 4, pp. 585–599, 2003.
- [28] J. Crétat, E. K. Vizy, and K. H. Cook, "The relationship between African easterly waves and daily rainfall over west Africa: observations and regional climate simulations," Climate Dynamics, vol. 44, no. 1-2, pp. 385–404, 2015.
- [29] S. Janicot, V. Moron, and B. Fontaine, "Sahel droughts and ENSO dynamics," *Geophysical Research Letters*, vol. 23, no. 5, pp. 515–518, 1996.
- [30] S. Janicot, "Impact of warm ENSO events on atmospheric circulation and convection over the tropical Atlantic and west Africa," *Annales Geophysicae*, vol. 15, no. 4, pp. 471–475, 1997.
- [31] G. Panthou, T. Vischel, and T. Lebel, "Recent trends in the regime of extreme rainfall in the central Sahel," *International Journal of Climatology*, vol. 34, no. 15, pp. 3998–4006, 2014.

- [32] H. Paeth, K. Born, R. Podzun, and D. Jacob, "Regional dynamical downscaling over west Africa: model evaluation and comparison of wet and dry years," *Meteorologische Zeitschrift*, vol. 14, no. 3, pp. 349–367, 2005.
- [33] D. J. Parker, Meteorology of Tropical West Africa: The Fore-casters' Handbook, p. 33, John Wiley & Sons, Hoboken, New Jersey, USA, 2017.
- [34] M. I. Lele and P. J. Lamb, "Variability of the intertropical front (ITF) and rainfall over the west African Sudan-sahel zone," *Journal of Climate*, vol. 23, no. 14, pp. 3984–4004, 2010.
- [35] C. Flamant, P. Knippertz, D. J. Parker et al., "The impact of a mesoscale convective system cold pool on the northward propagation of the intertropical discontinuity over west Africa," *Quarterly Journal of the Royal Meteorological Society*, vol. 135, no. 638, pp. 139–159, 2009.
- [36] T. O. Odekunle, "An assessment of the influence of the intertropical discontinuity on inter-annual rainfall characteristics in Nigeria," *Geographical Research*, vol. 48, no. 3, pp. 314–326, 2009
- [37] C. Mensah, L. K. Amekudzi, N. A. B. Klutse, J. N. A. Aryee, and K. Asare, "Comparison of rainy season onset, cessation and duration for Ghana from RegCM4 and GMet datasets," *Atmospheric and Climate Sciences*, vol. 6, no. 2, pp. 300–309, 2016
- [38] S. S. Vaidya and S. S. Singh, "Applying the betts-miller-janjic scheme of convection in prediction of the Indian monsoon," *Weather and Forecasting*, vol. 15, no. 3, pp. 349–356, 2000.
- [39] F. Mounier, S. Janicot, and G. N. Kiladis, "The west African monsoon dynamics. Part III: the quasi-biweekly zonal dipole," *Journal of Climate*, vol. 21, no. 9, pp. 1911–1928, 2008.
- [40] W. Ma, W. Huang, Z. Yang, B. Wang, D. Lin, and X. He, "Dynamic and thermodynamic factors associated with different precipitation regimes over south China during premonsoon season," *Atmosphere*, vol. 9, no. 6, 2018.
- [41] S. Minobe, A. Kuwano-Yoshida, N. Komori, S.-P. Xie, and R. J. Small, "Influence of the Gulf stream on the troposphere," *Nature*, vol. 452, no. 7184, pp. 206–209, 2008.
- [42] C. L. Ziegler, T. J. Lee, and R. A. Pielke, "Convective initiation at the dryline: a modeling study," *Monthly Weather Review*, vol. 125, no. 6, pp. 1001–1026, 1997.
- [43] S. Tajbakhsh, P. Ghafarian, and F. Sahraian, "Instability indices and forecasting thunderstorms: the case of 30 April 2009," *Natural Hazards and Earth System Sciences*, vol. 12, no. 2, pp. 403–413, 2012.
- [44] TT-DEWCE WMO, Guidelines on the Monitoring of Extreme Weather and Climate Events, Draft Version-First Review by TT-DEWCE, TT-DEWCE WMO, Geneva, Switzerland, 2015.